Communication

Caged Quantum Dots

Gang Han, Taleb Mokari, Caroline Ajo-Franklin, and Bruce E. Cohen

More About This Article

Additional resources and features associated with this article are available within the HTML version:

- Supporting Information
- Access to high resolution figures
- Links to articles and content related to this article
- Copyright permission to reproduce figures and/or text from this article

View the Full Text HTML

Caged Quantum Dots

Gang Han,[†,‡] Taleb Mokari,[‡] Caroline Ajo-Franklin,[†] and Bruce E. Cohen*,[†]

Biological Nanostructures and Inorganic Nanostructures Facilities, The Molecular Foundry, Lawrence Berkeley National Laboratory, Berkeley, California 94720

Received June 27, 2008; E-mail: becohen@lbl.gov

Photoactivatable organic fluorophores and fluorescent proteins (FPs) have been widely adopted for cellular imaging and have been critical for increasing temporal and spatial resolution,[1,2] as well as for the development of superresolution microscopy techniques.[3,4] Semiconducting nanocrystal quantum dots (QDs) possess superior brightness and photostability compared to either organic fluorophores or FPs but have not yet been engineered for microscopic photoactivation. As part of our efforts to develop nanoparticles with novel optical properties, we have synthesized photocaged quantum dots, which are nonluminescent under typical microscopic illumination but can be activated with stronger pulses of UV light.

ortho-Nitrobenzyl (ONB) groups have classically been used to cage biomolecules, rendering them inactive until pulsed with light.[5,6] UV irradiation induces a photolytic reaction, freeing the parent molecule along with a nitrosocarbonyl byproduct. With QDs, certain aromatic groups have previously been found to quench luminescence,[7,8] and we sought to determine whether ONB groups could do so until released photochemically (as shown in Figure 1).

CdTe/CdS core/shell QDs were grown under aqueous conditions in the presence of mercaptopropionic acid (MPA),[9,10] and lipoic acid-derived dithiolate ligands[11] were synthesized to contain an ONB-phosphoryl group. The phosphoryl group has proved to be an excellent substrate for caging groups[6] and possesses good aqueous solubility. The 4,5-dimethoxy-1-(2-nitrophenyl)ethyl (DM-NPE) caging group[12] absorbs at the longer UV wavelengths (ca. 355–413 nm) commonly used to photoswitch fluorescent proteins and produces a nitrosoketone byproduct (Figure 1) less toxic than those of other caging groups.

Mixtures of compound **3** (synthesized as shown in Scheme 1) and its noncaged analogue **4** were added to the nanoparticles and allowed to fully displace the monothiol MPA. Exchange occurred very rapidly, judging from an obvious loss of luminescence within the first few seconds upon mixing (not shown). This method of MPA displacement on water-grown QDs permits facile placement of varying percentages of caging groups onto the QD surface, as confirmed by their absorbance spectra[13] (Figure 2a). MPA displacement also permits the addition of other ligands for bioconjugation, cell compatibility, and targeting.[15]

Green CdTe/CdS QDs (λ_{max} = 520 nm) coated with 25% caged compound **3** showed a ca. 400-fold reduction in PL quantum yield compared to identical QDs coated with noncaged **4** (Figures 2b and S2a). By comparison, the difference between dark and bright states of PA-GFP is ca. 100-fold,[2] similar to the "fully quenched" state of dopamine-coated CdSe/ZnS QDs.[7] This contrast ratio is critical to imaging applications that require significant differences between dark and bright states.[4,16]

Exposure of caged QDs to 2 mW/mm² 365-nm light produced an increase in PL, as would accompany photolytic release of the
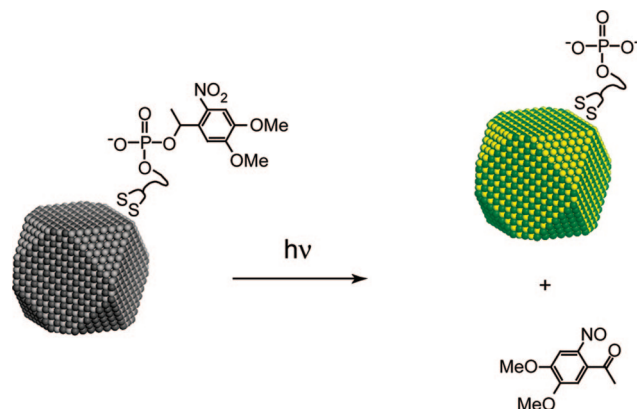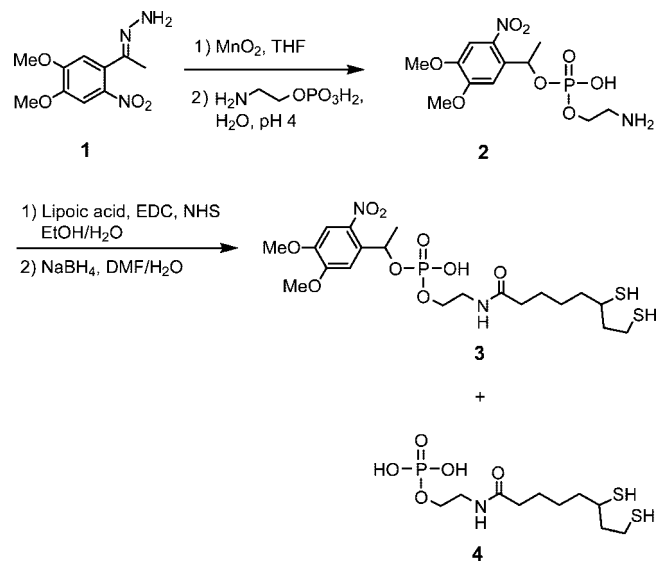

Figure 1. Quantum dot uncaging with *o*-nitrobenzyl ligands.

Scheme 1

ONB byproduct from the QD surface (Figure 2b–d). Noncaged QDs also typically displayed an increase in PL quantum yield upon UV exposure, though much smaller (ca. 1.3-fold) than that for the caged QDs, consistent with previous reports of photobrightening effects caused by the annealing of surface traps.[9,17] Longer illumination times led to full restoration of **3**-caged QD luminescence (Figures 2d and S2a), and at the longest times we consistently and unexpectedly observed caged CdTe QDs become brighter than their noncaged counterparts exposed to the same conditions. Photolysis also caused a small decrease in the size of these QDs in solution, from ca. 7 to 6 nm, as measured by dynamic light scattering (Figure S1).

We synthesized a second lipoic acid derivative **5** (Chart S1), with the ONB held fewer atoms from the QD surface than in
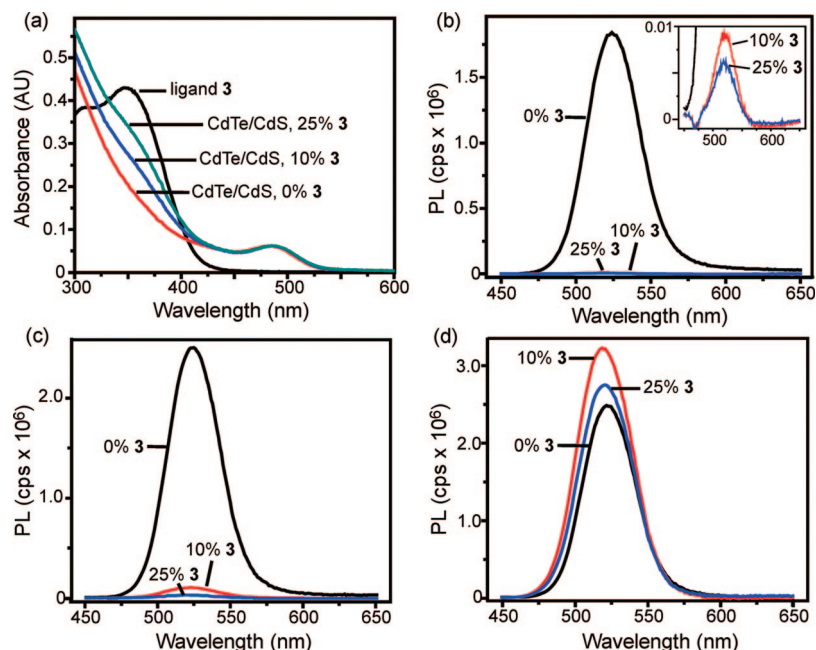
Figure 2. Optical characterization of QDs with varying percentages of surface ligand **3**. For all QDs, the remaining ligand is compound **4**. (a) Absorption spectra of green CdTe/CdS QDs and surface ligand alone. (b) PL spectra of CdTe/CdS QDs with ONB ligand **3**, excited at 405 nm. QD spectra are normalized to the absorbance at the first exciton. (c) PL spectra of QDs in Figure 2b following 2 min of 365-nm irradiation. (d) PL spectra of QDs in Figure 2b following 10 min of irradiation.
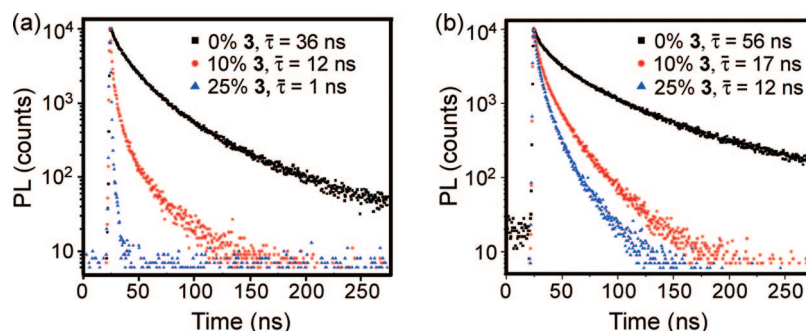

Figure 3. Transient PL emission detected with TCSPC, following 440-nm excitation of (a) green CdTe/CdS QDs (λ_{max} = 525 nm) and (b) red CdTe/CdS QDs (λ_{max} = 625 nm).

compound **3**. QDs coated with **5** showed consistently lower PL yields than QDs coated with similar fractions of **3** (Figure S2a), suggesting that the ONB−QD distance affects quenching efficiency. These QDs also underwent PL increases upon illumination, but less efficiently than QDs coated with **3**, possibly owing to the relatively poor uncaging ability of thiols compared to the phosphates.

We also sought to understand how ONB interacts with QDs of different compositions and emissions. Green InP/ZnS QDs (ref 14, λ_{max} = 524 nm) were quenched 30-fold by a 25% **3** surface coating (Figure S2b), about an order of magnitude less than comparable green CdTe/CdS QDs, possibly due to differences in shell thickness. Red CdTe/CdS QDs (λ_{max} = 625 nm) also displayed quenching by surface-bound ONB, though to a significantly lesser degree than the green QDs (Table S1). For near-infrared (nIR) CdHgTe/ZnS QDs (ref 17, λ_{max} = 760 nm), quenching was lesser still, about 25-fold, even with a 100% surface coating (Table S1). For all QDs, quenching increased with increasing fractions of surface ONB, although this effect saturated at a certain fraction. Importantly, we observe that ONB cages QDs over a wide spectral window, from green into the nIR.

One possible mechanism of ONB quenching would involve an inner filter effect, in which surface-bound ONB groups absorb

photons before they can reach the nanocrystal. We examined red CdTe/CdS ONB-coated QDs excited at the first exciton (Figure S2c), where ONB has no measurable absorbance (Figure 2a). These QDs still showed a decrease in PL quantum yield, but this decrease is less than that found with 405-nm excitation (Figure S2d). This reveals some inner filter effect, but the observed quenching with 605-nm excitation suggests the primary effect arises from an opticoelectronic coupling of the ONBs with the nanocrystal.

We therefore examined these red and green QDs with time-correlated single-photon counting spectroscopy (TCSPC) to determine if ONB affects the exciton lifetime (Figure 3). PL lifetimes of caged QDs were shorter than noncaged QDs, and the mean PL decay time decreased with increasing fraction of surface ONB, suggesting that ONB acts as a dynamic quencher of the exciton state. As with steady-state PL, this effect was more pronounced for QDs of shorter wavelength emissions. These shortened lifetimes are indicative of an electron or hole transfer from QD to ONB,[7,18] particularly since there is no overlap between QD emission and ONB absorption (Figure 2), excluding the possibility of exciton energy transfer.

To determine the cellular compatibility of caged QDs and their photolysis, we incubated green CdTe/CdS QDs coated with 10%
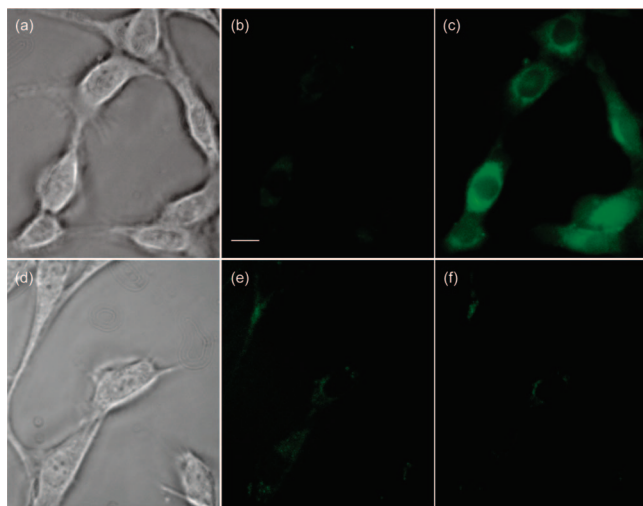
Figure 4. Live-cell imaging of QD uncaging. (a) Brightfield image of NIH 3T3 fibroblasts incubated with green CdTe/CdS QDs coated with 10% ligand **3**. Luminescent images of cells (b) before and (c) after photolysis with 387-nm light. (d) Brightfield, (e) prephotolysis, and (f) postphotolysis images of cells not incubated with caged QDs, irradiated, imaged, and processed identically with (a)−(c). Scale bar is 10 μm

ligand **3** with murine fibroblasts (Figure 4), which have previously been shown to endocytose QDs.[19] The remaining surface ligand was a mixture of positive and negative charges (compounds **6** (Chart S1) and **4**, respectively), which has been shown to minimize nonspecific QD adhesion to cell surfaces.[15] Before UV irradiation, little luminescence above cellular autofluorescence is visible (compare Figures 4b and 4e). Photolysis through the objective using the microscope Xe lamp and a 387-nm DAPI filter leads to a dramatic increase in perinuclear luminescence in cells with endocytosed caged QDs (Figure 4c), but not control cells (Figure 4f). Following uncaging, cells show no apparent changes in morphology, loss of adhesion, or other signs of toxicity from the photolysis or uncaging byproduct.

In summary, we have endowed quantum dots with one of the more useful properties of bioimaging probes: the ability to be switched on with light. The ONB caging group efficiently quenches QD luminescence and can be released from the nanoparticle surface with UV light. Caging is dependent on the emission of the QD but is observed through the visible spectrum into the nIR, offering a large array of new colors for photoactivatable probes. Like photoactivatable organic and FP probes, caged QDs can confer increased spatial and temporal resolution in biological imaging experiments, with the superior optical properties of QDs.

Supporting Information Available: Experimental procedures and figures, a chart, and a table. This material is available free of charge via the Internet at http://pubs.acs.org.

References

(1) (a) Mitchison, T. J.; Sawin, K. E.; Theriot, J. A.; Gee, K.; Mallavarapu, A. *Methods Enzymol.* **1998**, *291*, 63–78. (b) Ando, R.; Hama, H.; Yamamoto-Hino, M.; Mizuno, H.; Miyawaki, A. *Proc. Natl. Acad. Sci. U.S.A.* **2002**, *99*, 12651–12656.

(2) Patterson, G. H.; Lippincott-Schwartz, J. *Science* **2002**, *297*, 1873–1877.

(3) (a) Betzig, E.; Patterson, G. H.; Sougrat, R.; Lindwasser, O. W.; Olenych, S.; Bonifacino, J. S.; Davidson, M. W.; Lippincott-Schwartz, J.; Hess, H. F. *Science* **2006**, *313*, 1642–1645. (b) Moerner, W. E. *Proc. Natl. Acad. Sci. U.S.A.* **2007**, *104*, 12596–12602. (c) Hell, S. W. *Science* **2007**, *316*, 1153–1158. (d) Rust, M. J.; Bates, M.; Zhuang, X. W. *Nat. Methods* **2006**, *3*, 793–795.

(4) Shroff, H.; Galbraith, C. G.; Galbraith, J. A.; White, H.; Gillette, J.; Olenych, S.; Davidson, M. W.; Betzig, E. *Proc. Natl. Acad. Sci. U.S.A.* **2007**, *104*, 20308–20313.

(5) Mayer, G.; Heckel, A. *Angew. Chem., Int. Ed.* **2006**, *45*, 4900–4921.

(6) Mccray, J. A.; Trentham, D. R. *Annu. Rev. Biophys. Biol.* **1989**, *18*, 239–270.

(7) Clarke, S. J.; Hollmann, C. A.; Zhang, Z. J.; Suffern, D.; Bradforth, S. E.; Dimitrijevic, N. M.; Minarik, W. G.; Nadeau, J. L. *Nat. Mater.* **2006**, *5*, 409–417.

(8) (a) Yiidiz, I.; Tomasulo, M.; Raymo, F. M. *Proc. Natl. Acad. Sci. U.S.A.* **2006**, *103*, 11457–11460. (b) Huang, H.; Dorn, A.; Nair, G. P.; Bulovic, V.; Bawendi, M. G. *Nano Lett.* **2007**, *7*, 3781–3786. (c) Huang, J.; Stockwell, D.; Huang, Z.; Mohler, D. L.; Lian, T. Q. *J. Am. Chem. Soc.* **2008**, *130*, 5632–5633.

(9) Gaponik, N.; Talapin, D. V.; Rogach, A. L.; Hoppe, K.; Shevchenko, E. V.; Kornowski, A.; Eychmuller, A.; Weller, H. *J. Phys. Chem. B* **2002**, *106*, 7177–7185.

(10) Peng, H.; Zhang, L. J.; Soeller, C.; Travas-Sejdic, J. *J. Lumin.* **2007**, *127*, 721–726.

(11) Clapp, A. R.; Goldman, E. R.; Mattoussi, H. *Nat. Protoc.* **2006**, *1*, 1258–1266.

(12) Wilcox, M.; Viola, R. W.; Johnson, K. W.; Billington, A. P.; Carpenter, B. K.; Mccray, J. A.; Guzikowski, A. P.; Hess, G. P. *J. Org. Chem.* **1990**, *55*, 1585–1589.

(13) Based on the absorbance spectra in Figure 2a and literature values for the extinction coefficients of DMNPE[6] and CdTe QDs,[14] we estimate that the 10% caged 520-nm QDs have an average of 8 DMNPE groups per QD and the 25% caged QDs have 18, out of ca. 80 dithiolates per nanoparticle. Based on empirical calculations relating absorbance to particle size,[14] these particles have a 2 nm diameter and, assuming a spherical particle, a 12 nm² surface area. For 80 dithiolates, each will have a footprint of 0.15 nm², a physically reasonable value.

(14) Yu, W. W.; Qu, L. H.; Guo, W. Z.; Peng, X. G. *Chem. Mater.* **2003**, *15*, 2854–2860.

(15) Liu, W.; Howarth, M.; Greytak, A. B.; Zheng, Y.; Nocera, D. G.; Ting, A. Y.; Bawendi, M. G. *J. Am. Chem. Soc.* **2008**, *130*, 1274–1284.

(16) Certain imaging methods, such as PALM,[3a] also require that probes be photobleached following activation and imaging. While QDs have been shown to be more resistant to photobleaching than organic- and protein-based probes, they do indeed photobleach. For example, see : (a) Ma, J.; Chen, J. Y.; Zhang, Y.; Wang, P. N.; Guo, J.; Yang, W. L.; Wang, C. C. *J. Phys. Chem. B* **2007**, *111*, 12012–12016.

(17) (a) Jasieniak, J.; Mulvaney, P. *J. Am. Chem. Soc.* **2007**, *129*, 2841–2848. (b) Talapin, D. V.; Rogach, A. L.; Shevchenko, E. V.; Kornowski, A.; Haase, M.; Weller, H. *J. Am. Chem. Soc.* **2002**, *124*, 5782–5790.

(18) Jeong, S.; Achermann, M.; Nanda, J.; Lvanov, S.; Klimov, V. I.; Hollingsworth, J. A. *J. Am. Chem. Soc.* **2005**, *127*, 10126–10127.

(19) (a) Duan, H. W.; Nie, S. M. *J. Am. Chem. Soc.* **2007**, *129*, 3333–3338. (b) Jaiswal, J. K.; Mattoussi, H.; Mauro, J. M.; Simon, S. M. *Nat. Biotechnol.* **2003**, *21*, 47–51.

JA804948S